NYU

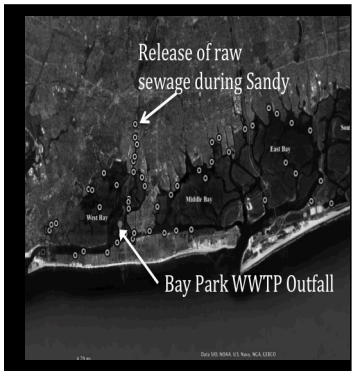

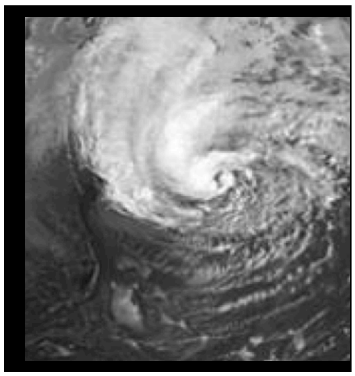

Stony Brook

NYS RISE

RESILIENCY INSTITUTE FOR STORMS & EMERGENCIES

SEA-LEVEL RISE IN NEW YORK IN THE 21ST CENTURY: PROJECTION AND METHODOLOGY

TR-0-15-01

MINGHUA ZHANG

May 2015

Table of Contents

Executive Summary

Based on the latest state-of-the-art sciences, this report calculated the sea-level rise (SLR) along the coasts of New York State (NYS) in 2100. Under the pessimistic greenhouse emission scenarios of RCP8.5, the upper bound SLR (95th percentile) in NYS is 50 inches relative to the reference period of 1986-2005; the projected medium value of SLR is 34 inches. Since our projection assumed the pessimistic climate change scenario, we conclude that SLR for NYS is very unlikely to be more than 50 inches by 2100.

SLR in this report is compared with projection by the New York City Panel on Climate Change (2015) that has much higher SLR of 75 inches for New York City (NYC) in 2100. The differences in the methodology and causes are discussed.

Introduction

This document describes the future projection of sea-level rise (SLR) by the New York State Resilience Institute for Storms and Emergencies (NYS RISE) based on our current knowledge of future climate change. It is prepared at the request of the NYS Department of Environmental Conservation (DEC). SLR along the coasts of Nassau and Suffolk is presented. The same SLR values may be also used for New York City (NYC) since current knowledge of future climate change is not sufficient to resolve SLR differences between Long Island and NYC. This document therefore refers to the region as either Nassau and Suffolk or New York (NY). Results in this report may be updated in the future as new information become available.

For the purpose of this report, SLR values are given relative to the average sea-level height in the reference period of 1986-2005. SLR projections are calculated for the climate change scenario Representative Concentration Pathway (RCP8.5) (IPCC, 2013). RCP8.5 resembles the scenario of "business-as-usual" emissions of greenhouse gases in the 21st Century in which radiative forcing to the atmosphere by anthropogenic greenhouse gases reaches 8.5 W/m2 at the end of the 21st Century. RCP8.5 is a plausible upper bound of emission scenarios that have been published in the literature (Van Vuuren et al., 2011). The RCP8.5 simulations are from the Coupled Model Intercomparison Project Phase 5 (CMIP5). They are available at the Earth System Grid data portal at http://cmip-pcmdi.llnl.gov/cmip5/data_portal.html. Simulations from 21 General Circulation Models (GCMs) are used. These models are described in the appendix of Zhang et al. (2014). Annual averages of the CMIP5 simulations are used in this report.

The report is organized as follows. Section 1 presents the projected SLR values for NY and for the global average, including mean values and upper bounds of the 90% range that brackets the 5th percentile and 95th percentile values. Section 2 describes the method and procedures of the SLR calculations. This section contains ten subsections, each of which describes the methodology of one individual process contributing to the total SLR. Section 3 describes the methodology of uncertainty estimates in the total SLR. An appendix is included about the observed past SLR in NY in the 20th Century to give a historical perspective for the future SLR.

Annual SLR and its contributions from each component, in terms of the mean, upper and low bounds, are provided as tabulated text files accessible from a web browser. Username and password are required to download the text data files since the results have not been formally published. Username and password can be obtained from the author upon request.

1. Projected SLR

SLR is calculated in this report by using process models. We consider the contributions from ten processes. This method is also used in the Fifth Assessment Report (AR5) by the Inter-governmental Panel for Climate Change (IPCC, 2013). The ten processes are:

1) Global Ocean Thermal Expansion (Thermosteric)
2) Melting of surface snow and ice in Greenland (Ice Sheet Mass Balance)
3) Melting of surface snow and ice in Antarctic (Ice Sheet Mass Balance)
4) Lateral discharge of ice from Greenland (Ice Sheet Dynamics)
5) Lateral discharge of ice in Antarctic (Ice Sheet Dynamics)
6) Melting of mountain glaciers
7) Anthropogenic extraction of groundwater
8) Glaciation Isostatic Adjustment (GIA)
9) Ocean dynamics
10) Change in sea level air pressure (SLP)

For the contribution of each process, the SLR ensemble mean and its upper/lower bounds of the 90% interval are calculated from an ensemble of models or methods. In the IPCC AR5 terminology: values outside the 5th and 95th percentile bounds are considered as "very unlikely" (IPCC 2013, Summary for Policymakers).

Table 1 below shows the projected upper 95th percentile of NY SLR in inches every 10 years in the 21st century relative to the reference period of 1986-2005 for the total SLR (**in red color**) and contributions from each of the individual components listed above in inches.

Year	Total (inch)	Greenland SMB	Antarctic SMB	Greenland Dyn	Antarctic Dyn	Glaciers	Ground Water	Thermo-steric	GIA	Ocean Dynamics	SLP
2020	**8.2**	0.1	-0.3	0.1	1.3	0.4	0.5	2.4	2.0	3.7	0.1
2030	**14.6**	0.2	-0.5	0.2	2.2	0.8	0.9	3.4	2.8	7.2	0.1
2040	**16.1**	0.3	-0.7	0.3	3.0	1.1	1.3	4.6	3.7	5.5	0.1
2050	**21.0**	0.4	-1.0	0.3	3.9	1.6	1.7	6.0	4.6	7.0	0.2
2060	**26.2**	0.6	-1.2	0.4	4.8	2.2	2.1	7.7	5.4	8.5	0.2
2070	**30.8**	1.0	-1.4	0.5	5.7	2.8	2.5	9.5	6.3	8.8	0.2
2080	**37.3**	1.4	-1.7	0.6	6.6	3.4	2.9	11.4	7.1	11.1	0.3
2090	**43.3**	1.9	-1.9	0.6	7.5	4.1	3.3	13.6	8.0	12.4	0.3
2100	**49.8**	2.6	-2.2	0.7	8.4	4.9	3.6	16.1	8.9	13.8	0.4

Table 1 (above). Projected upper 95th percentile of NY SLR under RCP8.5 climate change every 10 years in the 21st century (unit: inch) relative to the reference period of 1986-2005. The column in red is the total. Other columns are for the 10 individual processes. The sum of the 10 components is not the same as the total because the values in the table are the 95th percentile. Section 3 contains the explanations.

Figure 1.1 shows the mean, upper and lower bounds of SLR in NY under RCP8.5 climate change in feet. In 2100, the upper bound of SLR in NY is 4.1 feet; the mean value is 2.9 feet. The small fluctuations represent the internal variability of ocean circulations simulated by the GCMs. These fluctuations can be considered as random noise.

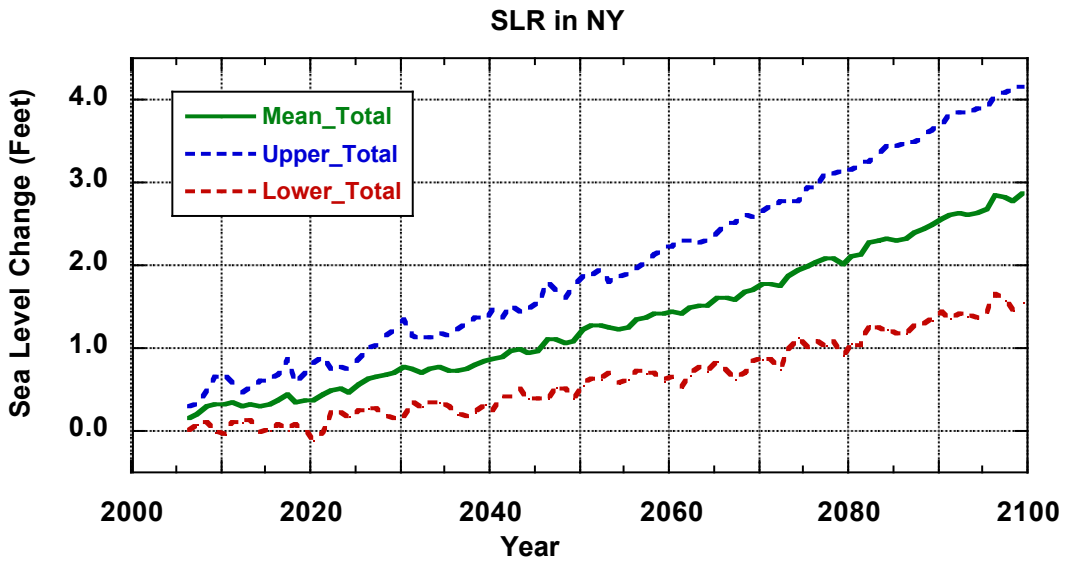

Figure 1.1 (above). Projected SLR in NY under RCP8.5 climate change scenario: mean (green), upper bound (95th percentile, blue), and lower bound (5th percentile, red).

The time series data in Figure 1.1 is available here. The values are slightly different from Zhang et al. (2014) where we interpolated the GCM data to 0.1^{o} by 0.1^{o} at monthly resolution and extrapolated them to the Nassau and Suffolk coasts separately. In this report, the GCM data are taken directly from the coarse model grids in the ocean that are closest to New York City.

As a comparison to NY SLR, the globally averaged SLR in the 21st Century is given in Figure 1.2. The upper bound of the global SLR is 3.4 feet; the mean value is 2.3 feet. SLR in NY is larger than the global value because of regional contributions from ocean currents, glaciation isostatic adjustment (GIA), and other factors that will be described in Section 3.

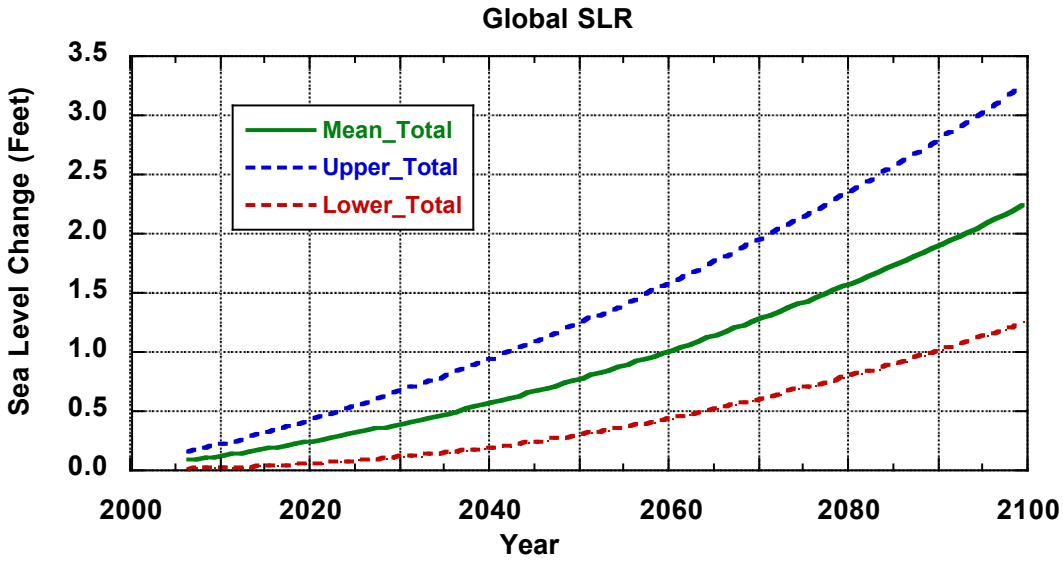

Figure 1.2 (above). Projected global SLR under RCP8.5 climate change scenario: mean (green), upper bound (95th percentile, blue), and lower bound (5th percentile, red).

The time series data in Figure 1.2 is available here.

Individual contributions of the ten processes to the 2100 upper 95th percentile NY SLR are shown in Figure 1.3. The largest contributor to the SLR is from the thermosteric effect of warmer ocean temperatures. This is followed by ocean circulation, Antarctic ice sheet dynamics, melting of glaciers, and GIA.

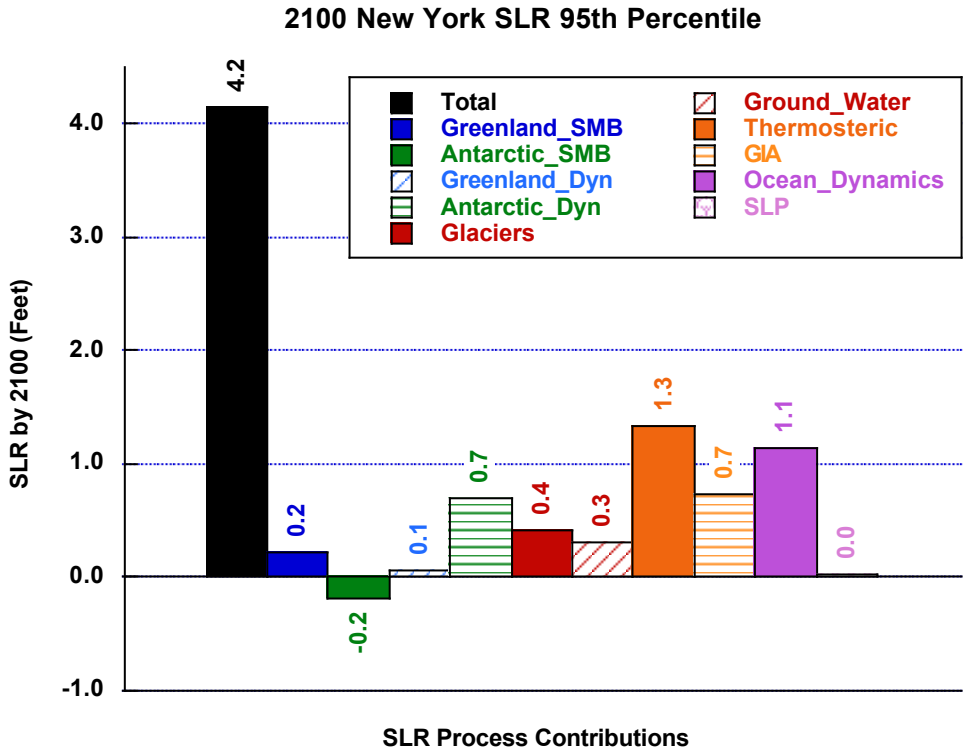

Figure 1.3 (above). 95th percentile values of projected 2100 SLR in NY under RCP8.5 climate change scenario: total (black) and each of the ten individual components described in the legend.

Individual contributions of the ten processes to the 2100 ensemble mean SLR are shown in Figure 1.4 for NY. The largest contributor to the SLR is from the thermosteric effect (38% = 1.1/2.9). The second largest contributor is ocean circulation (21% = 0.6/2.9). The next three contributors are Antarctic Ice Sheet Dynamics, melting of glaciers, and GIA (14%, 14%, and 10% respectively). The contribution of Surface Mass Balance (SMB) over Antarctic is negative to SLR, which is due to increased accumulation of surface snow there.

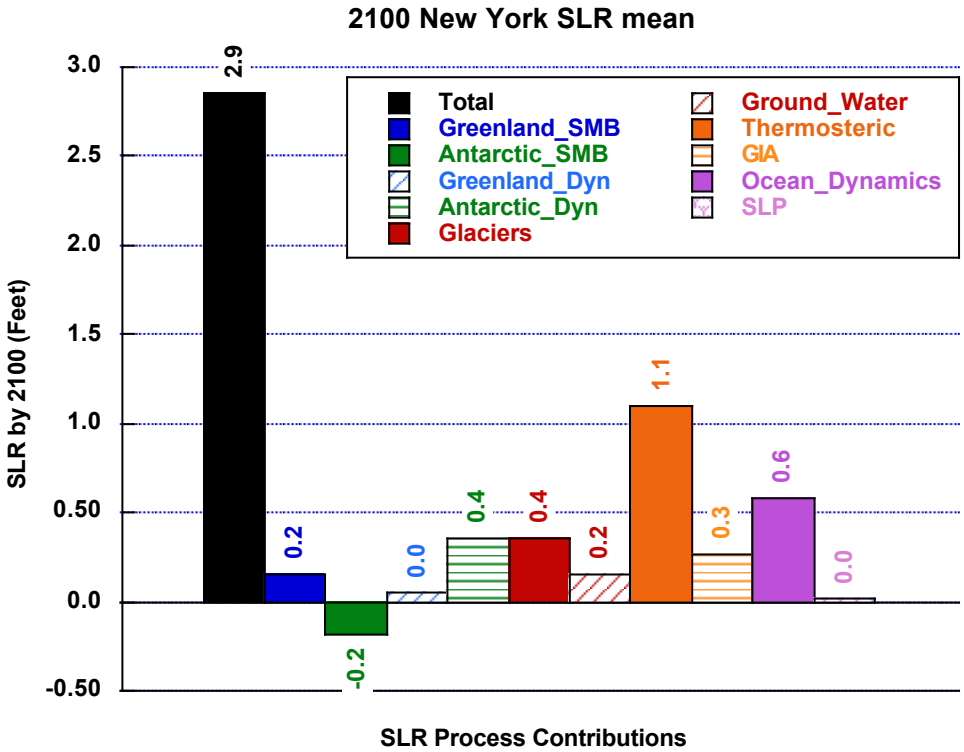

Figure 1.4 (above). Mean values of projected 2100 SLR in NY under RCP8.5 climate change scenario: total (black) and each of the ten individual components described in the legend.

As a comparison, the individual contributions of the processes to the 2100 ensemble mean SLR averaged over the world oceans are shown in Figure 1.5. The two leading contributors are the thermosteric effect and the melting of glaciers (45% = 1.0/2.2 and 27% = 0.6/2.2). These two processes account for about three thirds of the global SLR. The next two contributors are the melting of surface snow and ice over Greenland, and the dynamics of Antarctic Ice Sheet, each accounts for about 13% (0.3 feet) of global SLR.

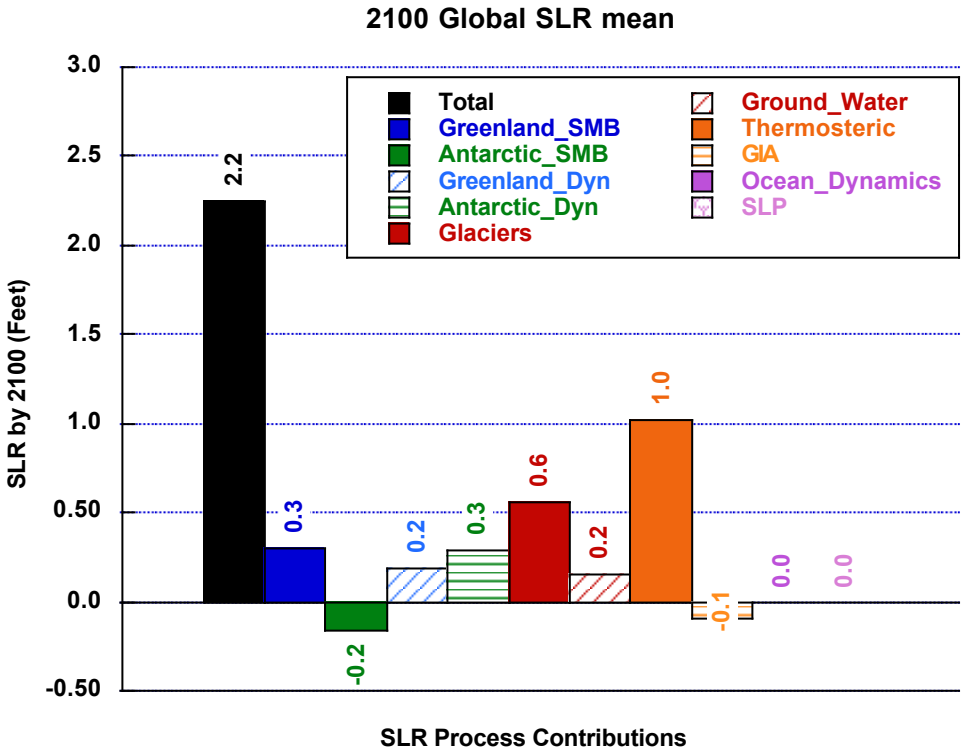

Figure 1.5 (above). Mean values of projected 2100 globally averaged SLR under RCP8.5 climate change scenario: total (black) and each of the ten individual components described in the legend.

It is noted that SLR of most individual processes for NY is different from the global averages. For example, ocean currents and GIA contribute to NY SLR, but they are negligible to global SLR. Greenland SMB and Ice Sheet Dynamics contribute a combined total of 0.5 feet (0.3+0.2) to the global SLR, but it is only 0.2 feet to NY SLR. This reduction of SLR is caused by the effect of rebalancing of the gravitational field when mass of snow and ice is lost in Greenland. Relaxation of the gravitational attraction of water near Greenland lowers the sea level in adjacent regions.

The gravitational effect of SLR caused by localized mass change on the Earth's surface (over the Greenland and the Antarctic, from melting of Glaciers and ground water change) is calculated by using the Sea-Level Equation (SLE) of Spada and Stocchi (2006). The SLE can be written as

$$\eta = \frac{\rho_i}{g} G_s \otimes_i \mathrm{I} + \frac{\rho_w}{g} G_s \otimes_o \eta + \eta^E - \overline{\frac{\rho_i}{g} G_s \otimes_i \mathrm{I}} - \overline{\frac{\rho_w}{g} G_s \otimes_o \eta} \qquad (1)$$

where η is the sea level height, I is the spatially distributed ice or snow mass, ρ_i and ρ_w are densities of ice and water, $\otimes_i$ and $\otimes_o$ are spatiotemporal convolutions over the varied frozen water mass and the ocean-covered regions, g is the gravity at the Earth's surface, and the last two ocean-averaged terms ensure mass conservation. The Green's function G_s is described in Spada and Stocchi (2006). The "eustatic term" η^E — the process term with net gain or loss of water mass in the oceans — represents the spatially uniform sea-level change for a rigid, non-gravitating Earth as shown by the individual globally averaged components in Figure 1.5. We used the time-dependent spatial distribution of sea level normalized by η^E that is solved from Equation (1) by Church et al. (2013).

Figure 1.6 shows an example of the normalized spatial distribution of SLR from the Greenland SMB. NY SLR from this process is only 52% of the global value in 2100 because of the relatively shorter distance of sea-level in NY than that in most of the oceans. For the Greenland Ice Sheet Dynamics, because the ice mass is mostly lost near the southern portion of the Greenland where the distance to NY is even smaller, NY SLR from the Greenland ice sheet dynamics is only 26% of the global mean (map not shown). The spatial distribution near North America in Figure 1.5 is similar to Figure 13.18(c) in IPCC AR5 that gave SLR from the combined changes of surface mass balance in Greenland and Antarctic (Church et al. 2013).

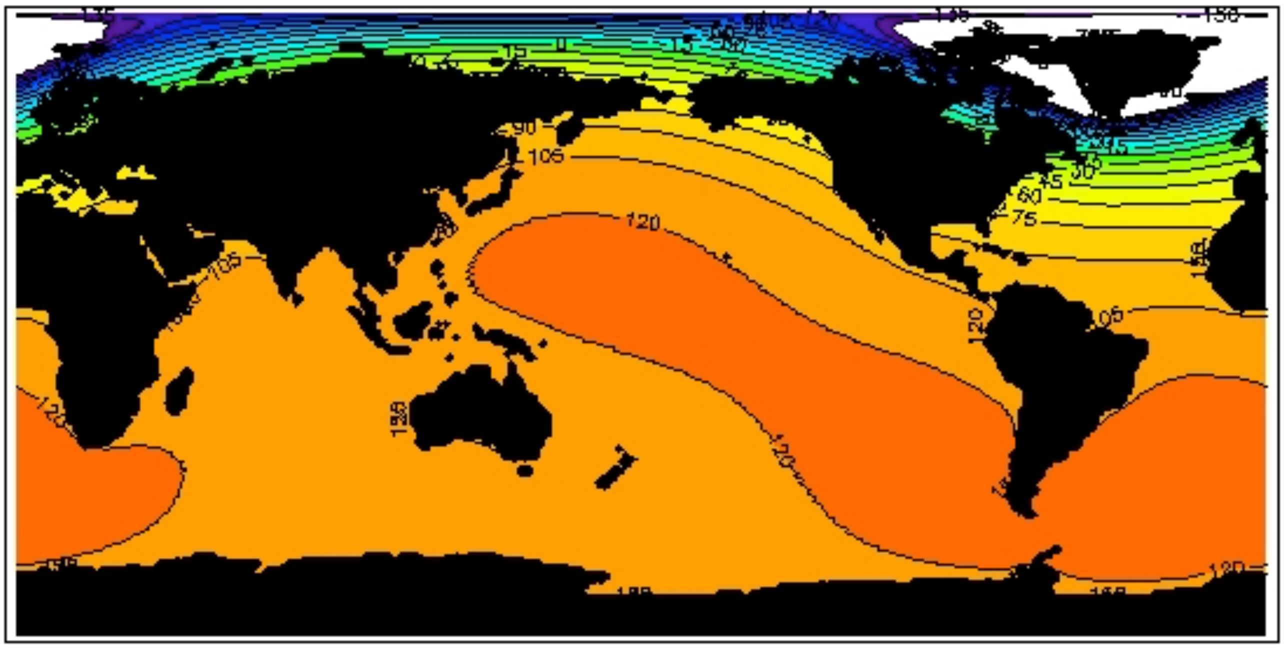

Figure 1.6 (above). Spatial distribution of the normalized percentage value of SLR relative to global mean from the melting surface snow and ice in Greenland in 2100.

2. Methodology of Process Calculations

2.1 Global Thermosteric SLR

The global thermosteric SLR represents the thermal expansion as a result of ocean warming. It is calculated by using the simulated change of ocean temperatures from the CMIP5 models.

The state equation of the ocean water is

$$\rho = \rho(T, S, p) \qquad (2)$$

where ρ is the density of seawater; T is temperature; S is salinity; p is water pressure. For a unit mass of seawater, the volume of seawater is

$$v = \frac{1}{\rho}.$$

Under climate change, the volume change of the seawater per unit mass is

$$\delta v = \delta\left(\frac{1}{\rho}\right) = -\frac{1}{\rho^2}\,\delta\rho = -\frac{1}{\rho^2}\,(\frac{\partial\rho}{\partial T}\delta T + \frac{\partial\rho}{\partial S}\delta S + \frac{\partial\rho}{\partial p}\delta p)$$

where δT, δS, and δp represent changes of climate.

The change of the total volume of seawater is

$$\Delta V = \iiint_{Oceans}(\delta v)\,(\rho dxdydz) = -\iiint_{Oceans}\left[\frac{1}{\rho}(\frac{\partial\rho}{\partial T}\delta T + \frac{\partial\rho}{\partial S}\delta S + \frac{\partial\rho}{\partial p}\delta p\right]dxdydz\,.$$

Because contributions from the changes of salinity and pressure changes are small, the following approximation can be made

$$\Delta V \approx -\iiint_{Oceans}\frac{1}{\rho}(\frac{\partial\rho}{\partial T}\delta T)dxdydz \qquad (3)$$

where

$$\frac{\partial\rho}{\partial T} \approx -\,\alpha(T, p) - \gamma(T, p)(35 - S)$$

and α, γ are calculated from the state equation (2).

Ensemble simulations of δT from 21coupled ocean-atmospheric General Circulation Models (AOGCMs) from RCP8.5 are used. Model drift of δT in the interior oceans is corrected as described in Church et al. (2013).

The SLR from the thermal expansion is calculated by

$$\delta\eta = \frac{\delta V}{A} \qquad (4)$$

where $\delta\eta$ is SLR, δV is from Equation (3); A is the total surface area of the oceans, taken to be 362.5×10^6 km2.

Figure 2.1 shows the ensemble average $\delta\eta$ and its upper/lower bounds. This term is the same for NY as for the global mean by definition. The annual time series data can be accessed here.

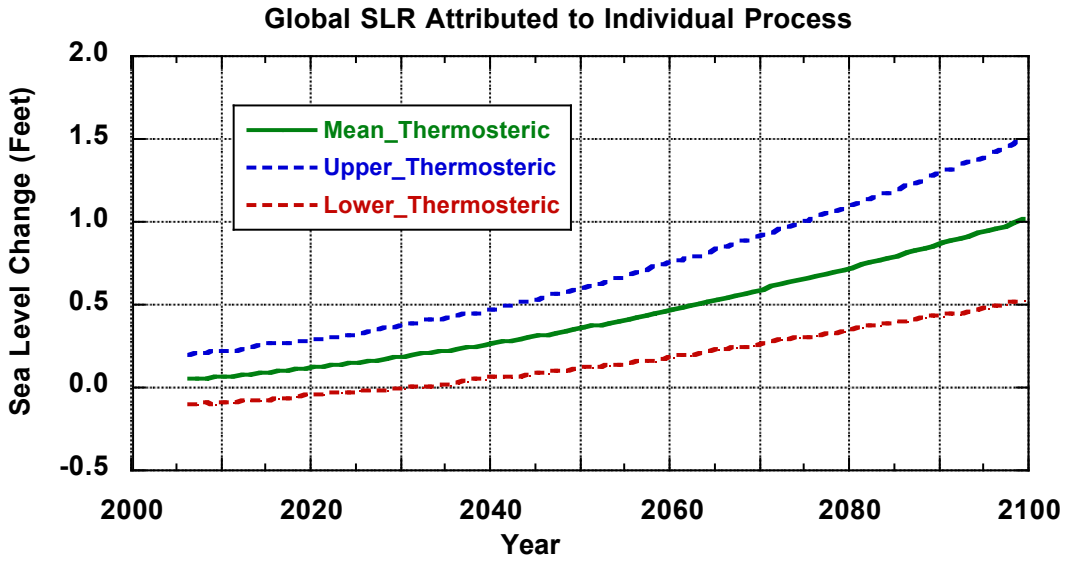

Figure 2.1 (above). SLR by global thermosteric contribution under RCP8.5 climate change scenario: mean (green), upper bound (95th percentile, blue), and lower bound (5th percentile, red).

2.2. Greenland SMB

Greenland will lose surface ice and snow as a result of melting due to warming. This causes sea level rise. Regional climate model simulate the net loss of mass from the melting and evaporation as well as precipitation. We used the model by Fettweis et al. (2013) to calculate the net mass loss as a function of global temperature:

$$LG = 71.5(\Delta T) + 20.4(\Delta T)^2 + 2.8(\Delta T)^3 \qquad (5)$$

where LG is the annual mass loss of surface frozen water over Greenland in Gt/year, ΔT is the anomaly of annual global surface air temperature in Kelvin degree relative to the mean of 1980-1999. ΔT is from the ensemble of RCP8.5 simulations of AOGCMs. Equation (5) was derived by fitting data from multiple regional climate models (Fettweis et al., 2013). IPCC AR5 used the same formula (Church et al., 2013).

The mass loss LG is converted to SLR by using the surface area of global oceans and water density. LG is multiplied by a constant of 1.2 to account for possible factors not included in regional climate models, such as the change of surface topography due to surface melting, as described in Church et al. (2013).

Figure 2.2 shows the NY SLR due to loss of Greenland surface mass along with its upper/lower bounds. The time series data in this figure can be accessed here.

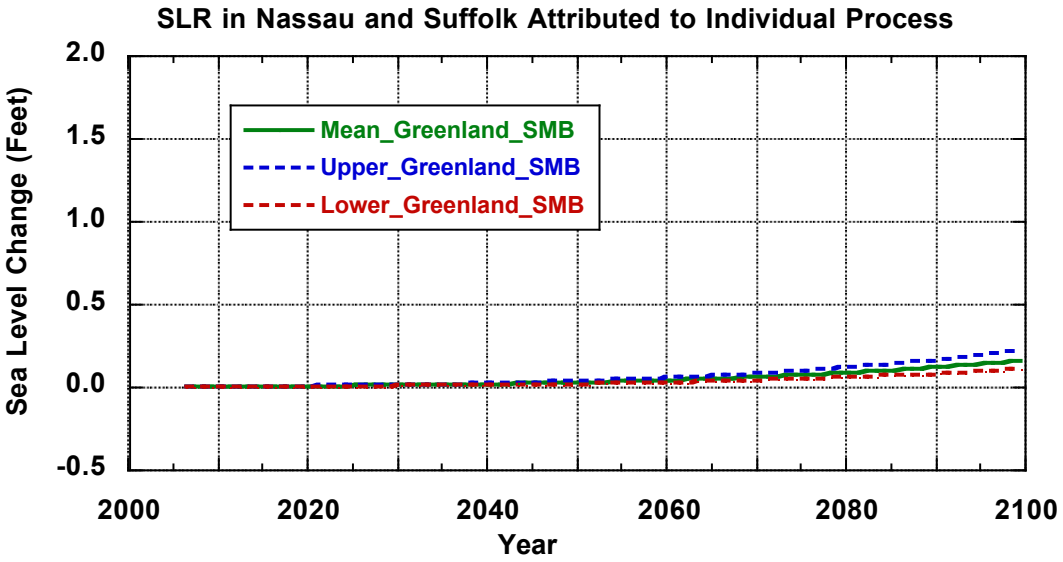

Figure 2.2 (above). SLR in NY due to mass loss of surface snow and ice in Greenland under RCP8.5 climate change scenario: mean (green), upper bound (95th percentile, blue), and lower bound (5th percentile, red).

As a comparison, Figure 2.2 shows the ensemble mean of global SLR due to loss of Greenland surface mass, along with its upper/lower bounds. The time series data in this figure can be accessed here.

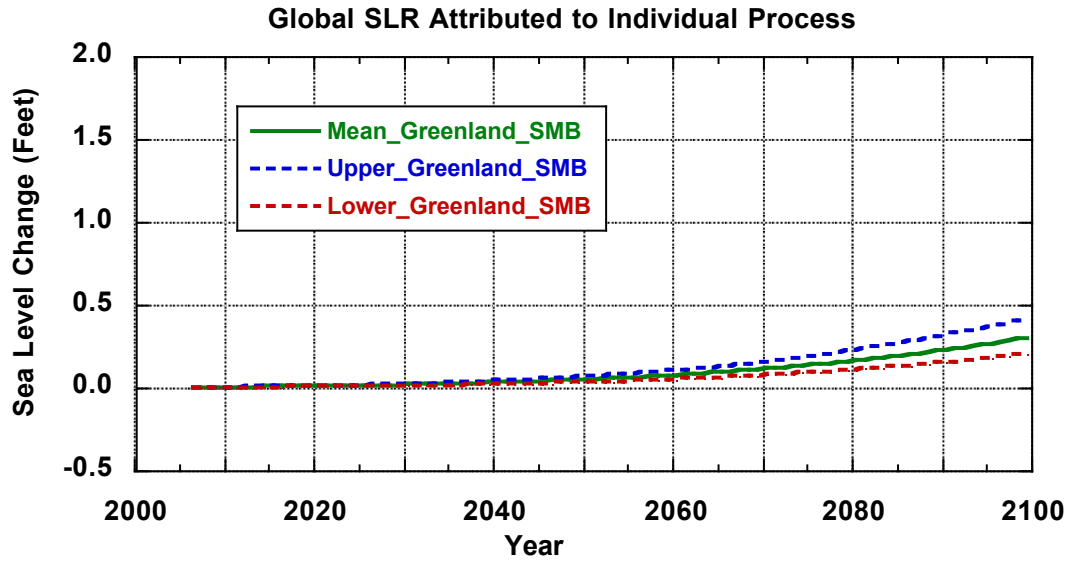

Figure 2.3 (above). SLR for the globe due to mass loss of surface snow and ice in Greenland under RCP8.5 climate change scenario: mean (green), upper bound (95th percentile, blue), and lower bound (5th percentile, red).

As discussed before, SLR in NY due to Greenland surface mass loss is smaller than that of the global average.

2.3. Antarctic SMB

Surface temperature over the Antarctic is below the freezing point in the 21st Century. Therefore, melting of surface snow or ice is not expected. Increased precipitation associated with atmospheric warming will lead to more snowfall over Antarctic and its accumulation. Snow accumulation causes net gain of ice mass over Antarctic and lowering of sea level.

We used the following formula to calculate the annual mass of total snowfall over Antarctic:

$$Snow(t) = Snow_0[1 + \frac{1}{Snow}(\frac{\partial Snow}{\partial T})\Delta T] \quad (6)$$

where ΔT is the anomaly of surface air temperature in Kelvin degree relative to the mean of the reference period 1985-2005. $Snow_0$ is 1923 Gt/year, which is the estimated annual snow amount in the reference period. The sensitivity of snow amount to temperature is taken based on Bengtsson et al. (2011) as:

$$\frac{1}{Snow}(\frac{\partial Snow}{\partial T}) = 5.1\% \text{ /K}$$

Only a fraction of the snowfall is retained on the surface because of the opposing side outflows and surface sublimation. Church et al. (2013) assessed the available literature and estimated the fraction of retained mass fraction to range from 0 to 35%. We used 10% to calculate the net snowfall accumulation as a conservative estimate of the lowering of the sea level from this process.

Figure 2.4 shows the ensemble average of NY SLR due to accumulation of Antarctic surface mass. The time series data in this figure can be accessed here. Values for the globe as a whole are similar and are not separately given here.

The small spread in the SLR is from different temperatures in the ensemble models. It is small since in Equation (6) the dominant factor is the snow amount in the reference period ($Snow_0$). The small spread only accounts for the uncertainty in temperature, not $Snow_0$and the fraction of retained net snow mass. The actual uncertainty accounting for these extra factors could be larger, but mostly to the negative SLR side, with negative upper bound.

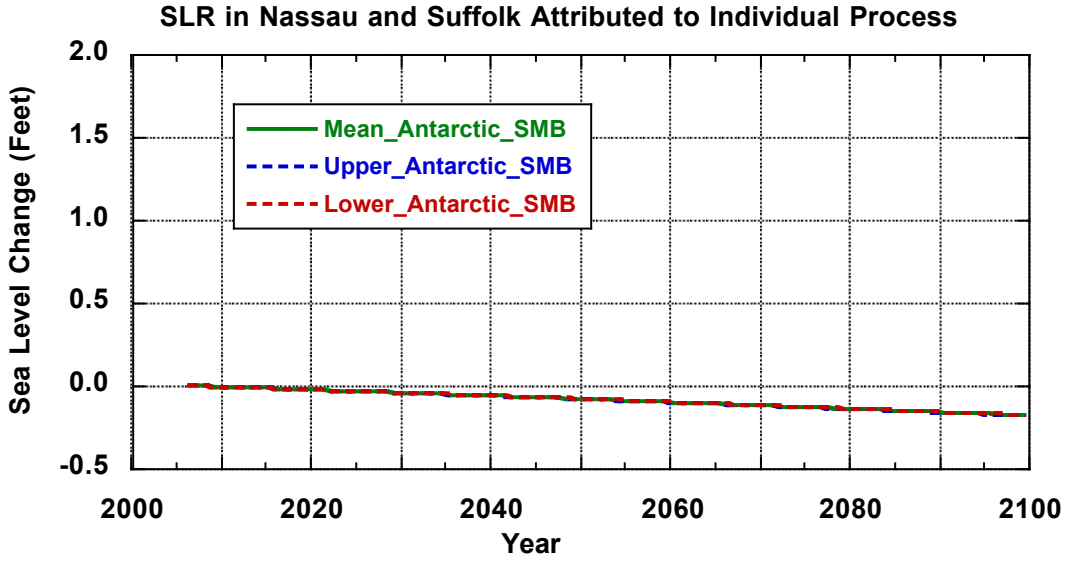

Figure 2.4 (above). SLR in NY due to mass loss of surface snow and ice in Antarctic under RCP8.5 climate change scenario: mean (green), upper bound (95th percentile, blue), and lower bound (5th percentile, red).

2.4 Greenland Ice Sheet Dynamics

SLR contribution from the periphery discharge of ice flow in southern Greenland is calculated by using a mean rate of 0.63 mm/year with a range of 0.46 to 0.80 mm/year. These annual rates are estimated by Vaughan et al. (2013) for the period of 2005-2009 based on 18 studies using satellite gravimetry, satellite altimetry, and mass budget analyses of the Greenland Ice Sheet.

Figure 2.5 shows the NY SLR due to Greenland ice sheet dynamics. The time series data in this figure can be accessed here.

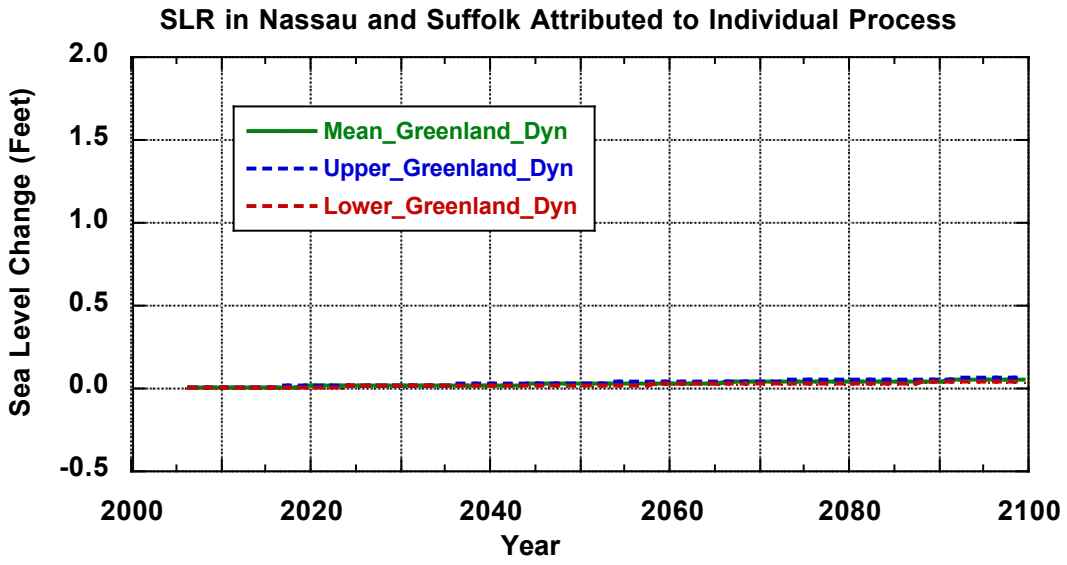

Figure 2.5 (above). SLR in NY due to periphery ice mass loss from Greenland ice sheet dynamics under RCP8.5 climate change scenario: mean (green), upper bound (95th percentile, blue), and lower bound (5th percentile, red).

As a comparison, Figure 2.6 shows the ensemble average of global SLR due to Greenland ice dynamics, along with its upper/lower bounds. As discussed before, SLR in NY due to Greenland ice loss is much smaller than that of the global average. The time series data in Figure 2.6 can be accessed here.

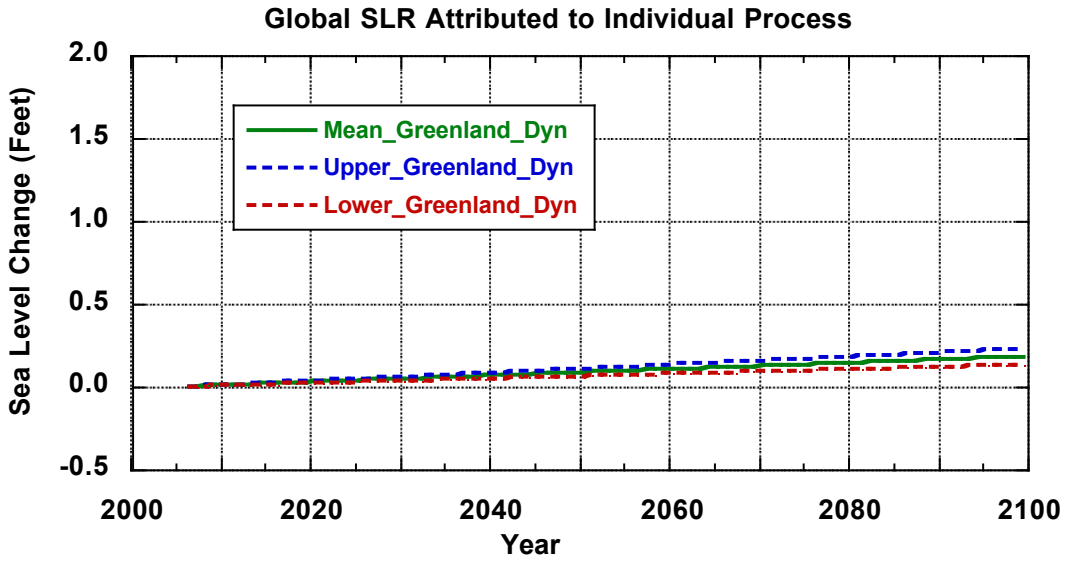

Figure 2.6 (above). SLR of the global ocean due to periphery ice mass loss from Greenland ice sheet dynamics under RCP8.5 climate change scenario: mean (green), upper bound (95th percentile, blue), and lower bound (5th percentile, red).

2.5 Antarctic Ice Sheet Dynamic Flow

SLR contribution from Antarctic ice discharge is calculated by using a mean rate of 0.985 mm/year with a range of 0 to 1.97 mm/year. The upper bound was based on the upper 95th percentile value in Little et al. (2013) who calculated the ice discharges of eighteen drainage basins in Antarctic for the 21st Century by using a combination of ice sheet models, energy balance models, and historical trends. The lower bound is a zero cut-off to the 5th percentile negative value in Little et al. (2013). The upper bound corresponds to 716.4 Gt annual loss of Antarctic ice.

Figure 2.7 shows the SLR in NY due to Antarctic ice sheet dynamics, along with its upper/lower bounds. The time series data in this figure can be accessed here. Values for the globe as a whole are similar and are not separately given.

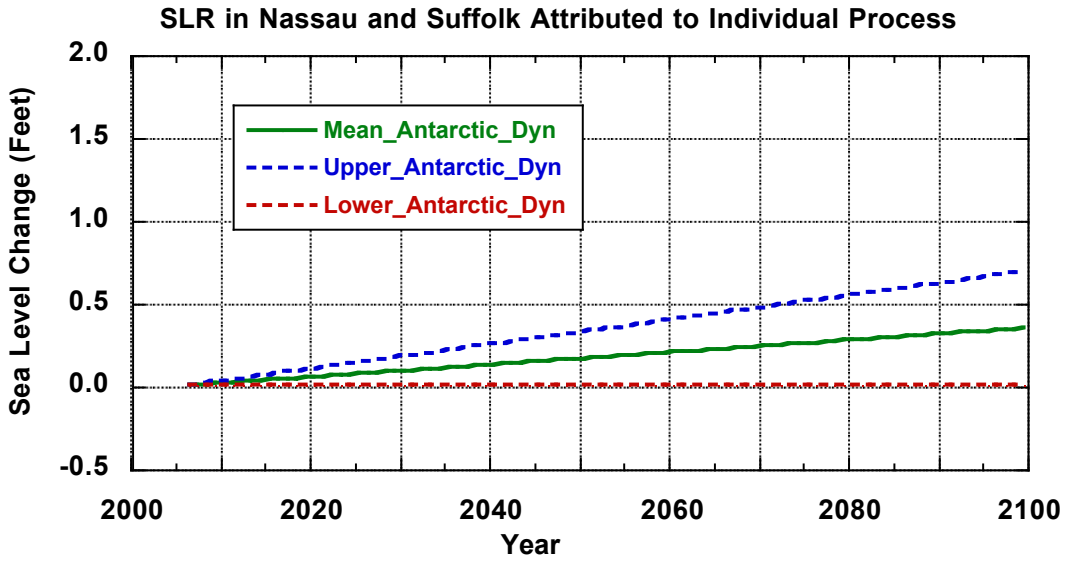

Figure 2.7 (above). SLR in NY due to periphery ice mass loss from Antarctic ice sheet dynamics under RCP8.5 climate change scenario: mean (green), upper bound (95th percentile, blue), and lower bound (5th percentile, red).

2.6 Melting of Glaciers

In glaciology, the mass of a glacier is often written as

$$M = \rho_i \, cA^{\gamma}$$

where A is the surface area of the glacier, ρ_i is the ice density, c and γ are geometric scaling factors with γ between 1.0 to 1.5. Several studies have calculated the mass change of mountain glaciers in 19 regions around the world (e.g., Radic and Hock, 2011). Aggregating results of all glaciers from four such studies, Church et al. (2013) used the following formula to calculate the net mass loss of glaciers as a function of global temperature anomaly:

$$L = \alpha(\int_{2006}^{t} \Delta T \, dt)^{\beta} \qquad (8)$$

where ΔT is the temperature anomaly in Kelvin degrees relative to 2006, α and β are fitting constants. We used Equation (8) and α = 1536 Gt/year, β = 0.71. The α and β values are the mean values in Church et al. (2013).

Figure 2.8 shows the ensemble average NY SLR due to loss of glacier mass. The time series data in this figure can be accessed here. Values for the globe as a whole are about 50% larger because the glaciers are located mostly in the polar regions that are closer to NY than to the global oceans.

The spread in this figure only accounts for the uncertainty in temperatures from the ensemble of RCP8.5 CMIP5 simulations. Uncertainties from the methodology are not quantified.

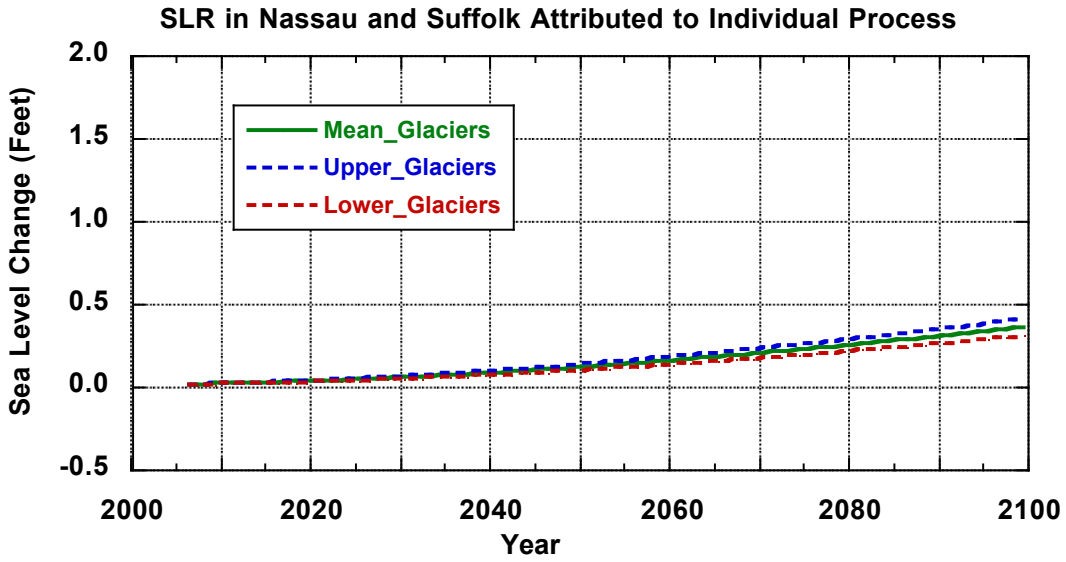

Figure 2.8 (above). SLR in NY due to glacier mass loss under RCP8.5 climate change scenario: mean (green), upper bound (95th percentile, blue), and lower bound (5th percentile, red).

2.7 Ground Water Storage Change

Anthropogenic extraction of groundwater can lead to SLR. We used the rate of 0.53 mm/year with an uncertainty range of 0 to 1.06 mm/year SLR. This range brackets the total range of 0.18 to 0.96 mm/year estimated in Konikow (2011) and Wada et al. (2012). The Konikow (2011) study calculated the volume change of groundwater in the 20th Century by using a combination of aquifer measurements, hydrological modeling, and satellite gravity measurents. The Wade et al. study (2012) used past country-based groundwater abstraction trends from the International Groundwater Resources Assessment Center Century (IGRAC) database (http://www.un-igrac.org/) and social-economic and climate simulations for the 21st Century.

NY SLR due to anthropogenic extraction of groundwater is shown in Figure 2.9. The time series in this figure can be accessed here. Values for the globe as a whole are similar and are not separately given.

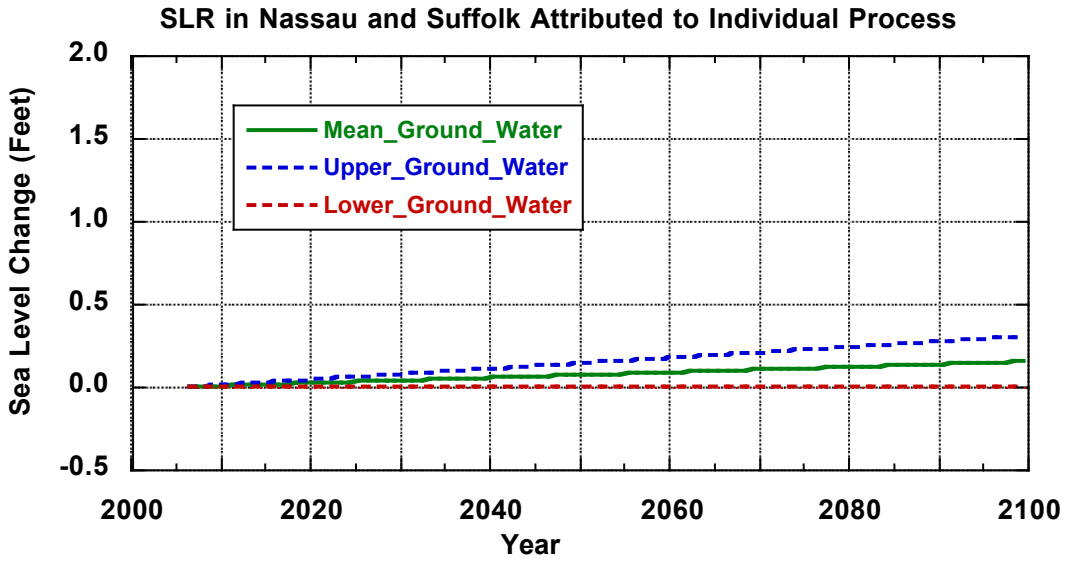

Figure 2.9 (above). SLR in NY due to anthropogenic use of groundwater: mean (green), upper bound (95th percentile, blue), and lower bound (5th percentile, red).

2.8 Glaciation Isostatic Adjustment (GIA)

GIA refers to the rebounding of the interior continents after ice melted from the last glaciation. The rebounding of the interior continent causes relative SLR along the coasts. The GIA calculation uses the same Sea-Level Equation as (1). Different assumptions can be made on the history of the deglaciation and the physical properties of the earth. We used the average of two datasets calculated by Lambeck et al. (1998) and by Peltier (2004) as our mean, and the absolute value of their differences with the mean as the standard deviation. This approach is also used in Church et al. (2013).

SLR from GIA in NY is shown in Figure 2.10. The time series data in this figure can be accessed here. The spread in the figure is larger than the difference between the two datasets by a factor of 1.645 since the spread represents the 5th and 95th percentiles.

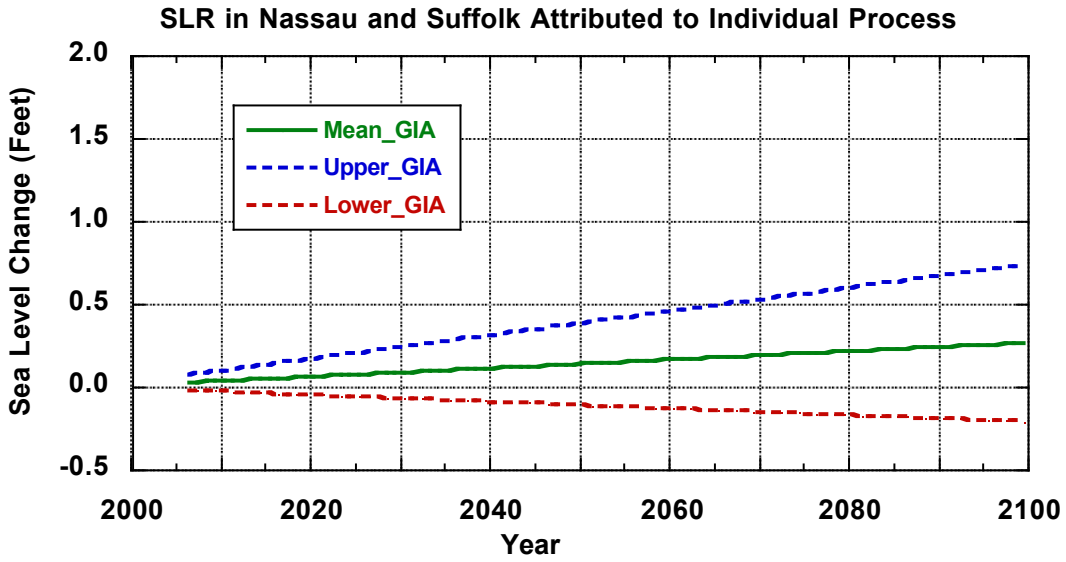

Figure 2.10 (above). SLR in NY due to Glaciation Isostatic Adjustment: mean (green), upper bound (95th percentile, blue), and lower bound (5th percentile, red).

2.9 Ocean Dynamics

Sea surface height (SSH) η, labeled the 'zos' variable in the CMIP5 archive, is obtained from the CMIP5 AOGCM database. In GCMs, the height is calculated from the mass continuity equation of the water column written as

$$\frac{\partial \eta}{\partial t} = -\nabla \cdot \left[(\mathrm{H} + \eta) \vec{\bar{V}} \right] + q_w \qquad (9)$$

where H is the local distance of the global mean sea level relative to the local bottom ocean floor, η is the local sea level height relative to the global mean, $\vec{\bar{V}}$ is the vertically integrated ocean current over a local water column, q_w is the freshwater flux to the ocean. $q_w$has been separately considered in this report. The spatial distribution of η therefore depends on the currents, which are in turn related to horizontal heterogeneity of temperature and salinity in the oceans. As climate changes, the ocean circulation changes. This causes the spatial structure of SLR from ocean dynamics.

We removed the global mean of η from each model to exclude the global thermosteric effect that has been separately calculated and possible model drift.

All SLR data presented so far are annual averages. SLR is preferably calculated for the month of its maximum during a year. We therefore added the amplitude of the seasonal variation of η for each model in NY coast to η. This is taken as 25.4 mm by 2100.

NY SLR from ocean dynamics is shown in Figure 2.11. The time series data in this figure can be accessed here. The large spread reflects the range of internal variability of the ocean GCMs.

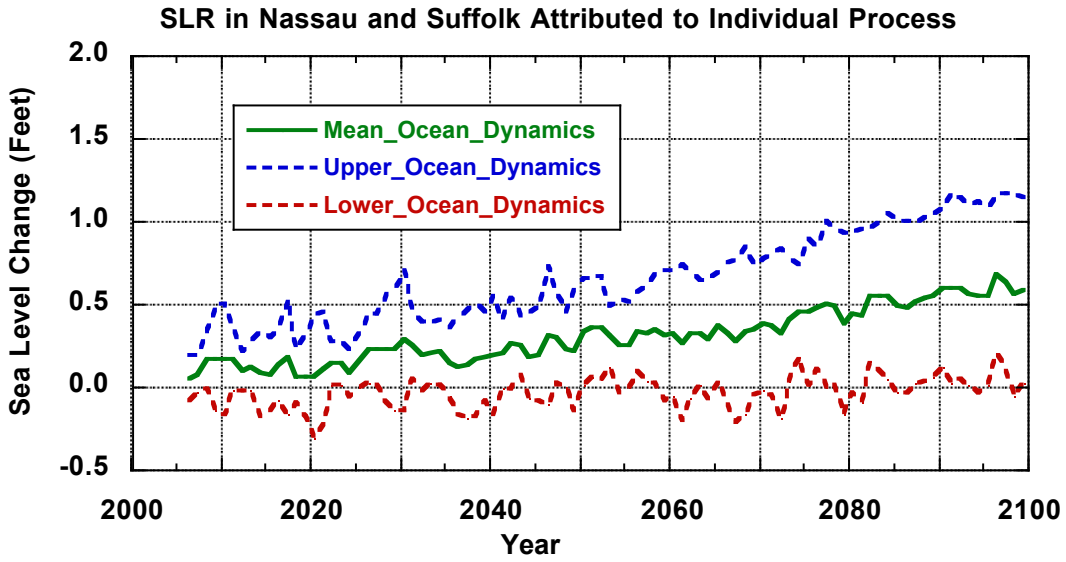

Figure 2.11 (above). SLR in NY due to changes in ocean dynamics under the RCP8.5 climate change scanario: mean (green), upper bound (95th percentile, blue), and lower bound (5th percentile, red).

2.10 Change in Sea Level Pressure (SLP)

Changes in surface pressure patterns will cause local sea level to rise or fall. We used the following hydrostatic equation to calculate this effect based on CMIP5 ensemble simulations of changes in sea level air pressure.

$$\Delta h = -\Delta P_s/(\rho_w g) \qquad (8)$$

where ΔP_s is the change of local sea level air pressure, ρ_w is the density of seawater in at 1029 kg/m3, g is the surface gravity at 9.8 m/s2. Redistribution of the gravitational field is not considered since the impact is very small.

Based on CMIP5 model simulations, we used ΔP_s = - 50 Pa (N/m2) with a range of -100 to 0 Pa near the NY coasts at the end of the 21st Century. This leads to Δh of 0 to 10 mm. This effect is therefore negligible for NY and so it is not plotted here.

3. Summation and Uncertainties

The ensemble means of the projected total SLR in NY and its ten process components are shown in Figure 3.1. The total SLR is the sum of all ten process terms. Consistent with Figure 1.4 in Section 2, the dominant contribution is from the global thermosteric effect. The next leading contributions are from the change of ocean circulations, melting of glaciers, and Antarctic ice sheet dynamics.

In our calculations, the rate of change is a function of time only for processes that are explicitly related with surface temperature. These include thermal expansion, Greenland and Antarctic surface mass budgets, glaciers and ocean dynamics. For other processes, constant rates are assumed for the 21st

Century. These processes include the dynamics of Greenland and Antarctic ice sheets, groundwater effect, GIA, and surface pressure effect. This linear assumption for the ice dynamics terms may have overestimated the rate in the first half of the 21st Century and underestimated the rate in the second half of the century. But it would not impact the result at the end of the 21st Century.

The time series in Figure 3.1 can be accessed here.

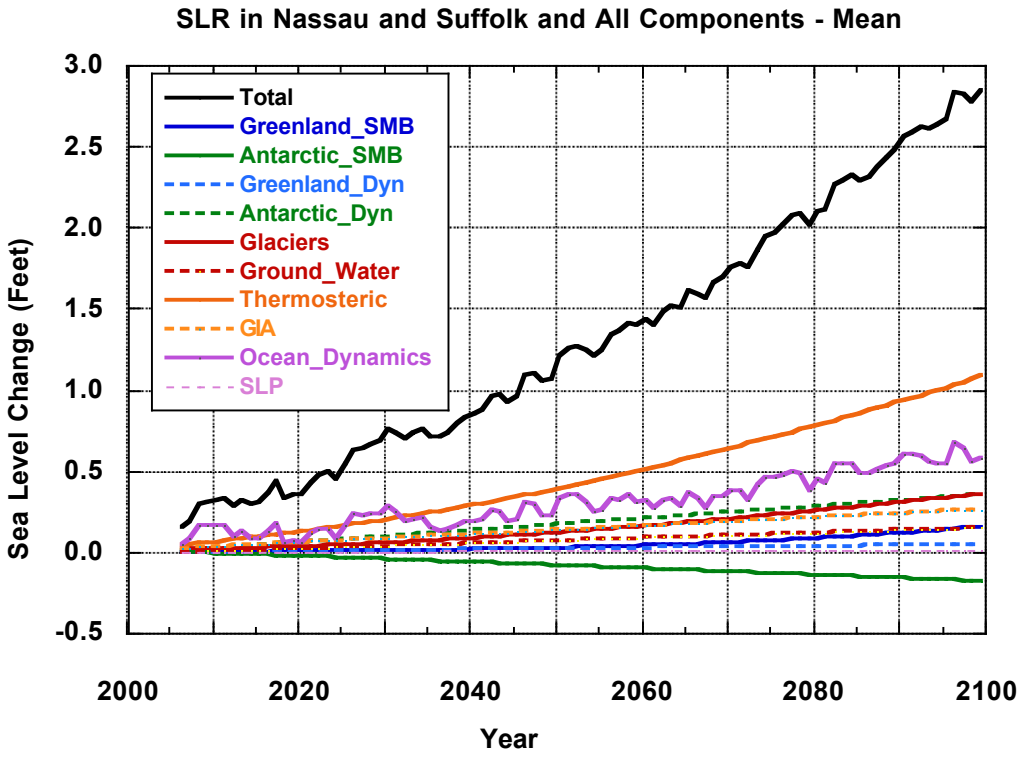

Figure 3.1 (above). Ensemble means of the total SLR in NY (black) and its ten contributing processes (see legend for process names) under the RCP8.5 climate change scenario

The ensemble upper bound (95th percentile) of the projected total SLR in NY and the upper bounds of its ten process components are shown in Figure 3.2. The time series data can be accessed here.

In calculating the upper bound of the total SLR, we assumed that errors in the following eight components are perfectly correlated: thermal expansion, surface mass balance in Greenland and Antarctic, ice sheet dynamics in Greenland and Antarctic, melting of glaciers, and ocean dynamics, and surface pressure effect. Uncertainties in these eight components are therefore additive. This assumption considers global climate warming as the common driver of all these terms. It maximally accumulates the uncertainty range of the total SLR. It compensates for the possible underestimation of uncertainty range of the individual terms where we only considered the temperature uncertainties without considering methodology uncertainties. Uncertainties from groundwater extraction and GIA are taken as independent random variables. The processes uncertainties are therefore combined together through the following equation:

$$\sigma_{sum} = \sqrt{(\sum_{i=1}^{i=8} \sigma_i)^2 + \sigma_{GW}^2 + \sigma_{GIA}^2} \qquad (10)$$

where σ_i is the standard deviation for each of the eight processes described before, σ_{GW} is the standard deviation of the groundwater effect, and σ_{GIA} is the standard deviation of the GIA term. The total upper bound in Figure 3.2 is therefore not the simple sum of the upper bounds of the ten component terms.

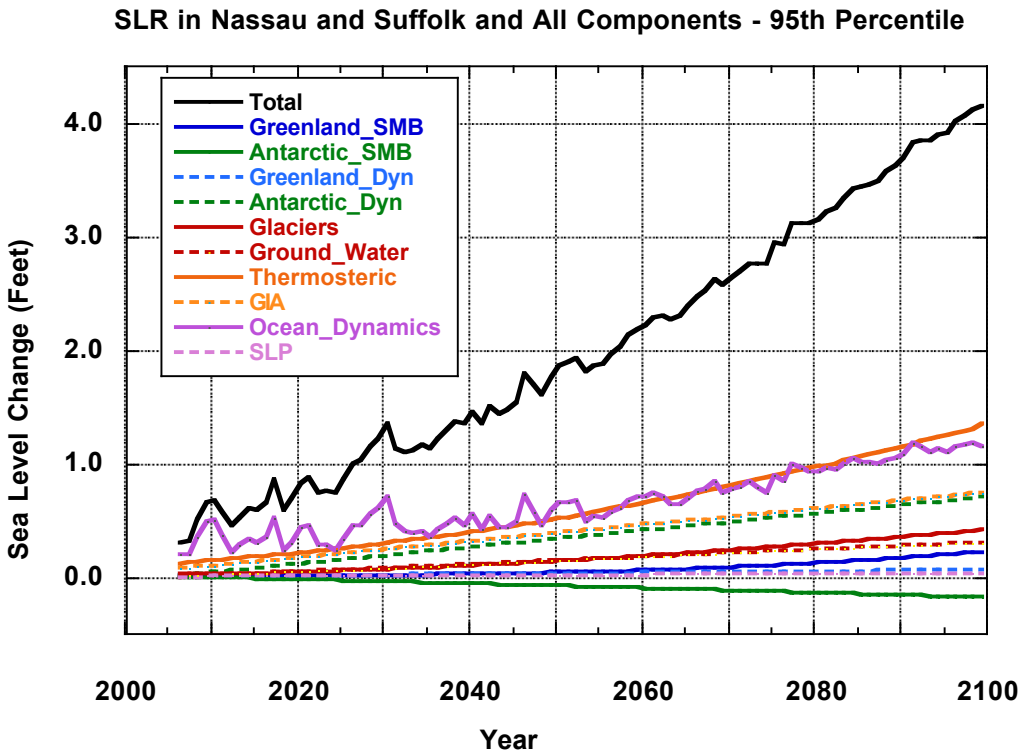

Figure 3.2 (above). Ensemble upper bound (95th percentile) of the total SLR in NY (black) and the upper bounds of the ten contributing processes (see legend for process names) under the RCP8.5 climate change scenario

4. Comparison with Other Studies

IPCC AR5

The SLR projected in this report is slightly larger than the results in the IPCC AR5 (IPCC 2014). In its report (Figure 13.23, page 1198), IPCC projected SLR for several large cities including San Francisco and NYC in relative to the same base period of 1986 to 2005. Figure 4.1 below shows the time series and the 5th to 95th percentile range of NYC SLR projection from the low emission RCP4.5 climate change scenarios in IPCC AR5. The 5th to 95th percentile ranges of projection for RCP2.6, RCP4.5, and RCP8.5 scenarios in 2100 are shown as colored bars on the left of each panel, with the red line describing the high emission RCP8.5 scenario. For NYC, the 95th percentile SLR in 2100 for NYC under scenario of the RCP8.5 climate change is 1.2 meter or 47 inches, 3 inches smaller than the 50 inches we projected in this report. This

small difference between NYC RISE projection and IPCC AR5 can be partially attributed to the different assumptions on how errors are correlated with each other among different components.

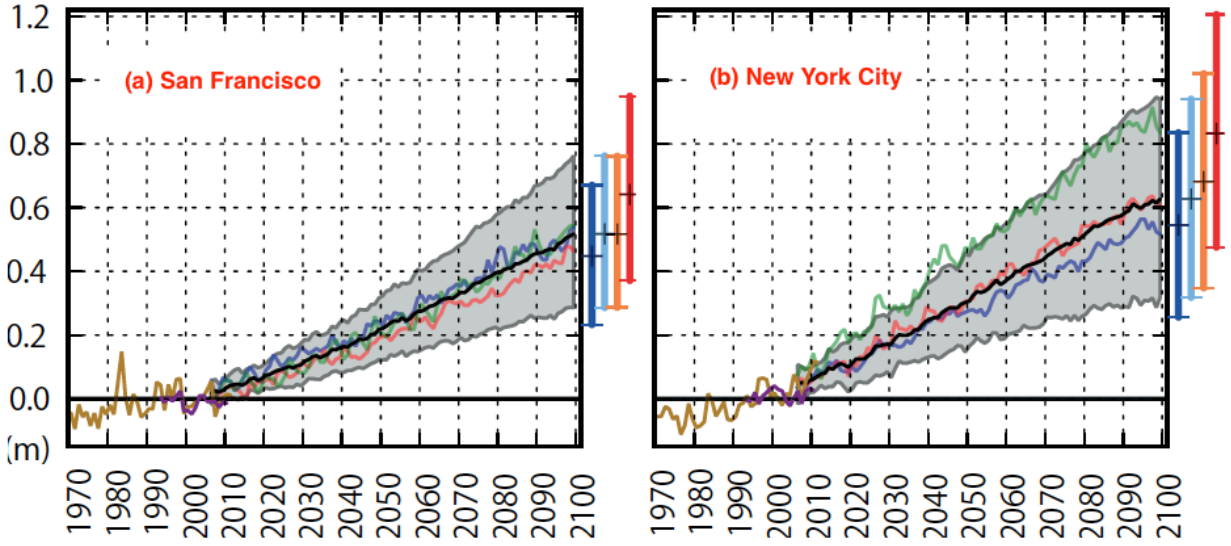

Figure 4.1 | Observed and projected relative sea level change for San Francisco and NYC by IPCC AR5 (2014). The projected range from 21 CMIP5 RCP4.5 scenario runs (90% uncertainty) is shown by the shaded region for the period 2006–2100, with the bold line showing the ensemble mean. Colored lines represent three individual climate model realizations drawn randomly from three different climate models used in the ensemble. Vertical bars at the right sides of each panel represent the ensemble mean and ensemble spread (5 to 95%) of the likely (medium confidence) sea level change at each respective location at the year 2100 inferred from RCPs 2.6 (dark blue), 4.5 (light blue), 6.0 (yellow) and 8.5 (red). (Figure from IPCC AR5, 2014)

New York City Panel on Climate Change (NPCC, 2015)

The New York City Panel on Climate Change (NPCC 2015, Horton et al. 2015) projected the 90th percentile upper bound of SLR in NYC to be 75 inches. This is considerably larger than the 95th upper bound of 50 inch SLR in this report. If the 95th percentile threshold were used, the NPCC (2015) projection would be larger than 75 inches. The difference is caused primarily by the calculation of SLR due to ice loss from the Greenland Ice and Antarctic Ice Sheets.

The ice sheet contribution to SLR in the NPCC (2015) was based on the expert survey by Bamber and Aspinall (2013) (referred to as BA13). The BA13 survey got 13 responses, and as BA13 said, one of the 13 responses was an outlier:

> "Examination of the range plots (Supplementary Fig. S7) indicates a substantial increase in the upper limit for the contribution of the WAIS (West Antarctic Ice Sheet) from one survey to the next (10.5-16.9mmyr^{-1}), but with the expected central value remaining almost unchanged."

The referred supplementary Fig. S7 of BA13 is appended below. In this figure, the red lines denote the range of the SLR rate from the 2012 survey that BA13 used; the letter "M" denotes response from a modeler; "O" denotes an observational expert. The outlier is from one of the modelers, who gave a low SLR rate value in a 2010 survey but very large range in the 2012 survey. Also shown in Fig. S7 are the pooled solutions in which the 13 surveys are weights in three ways. BA13 acknowledged that the upper bound in the paper was caused by one outlier response from the survey. This outlier significantly skewed the upper bound of the pooled solutions in the figure, even though the medium value is little affected. NPCC (2015) relied on the upper bound of BA13 in its SLR projection for NYC.

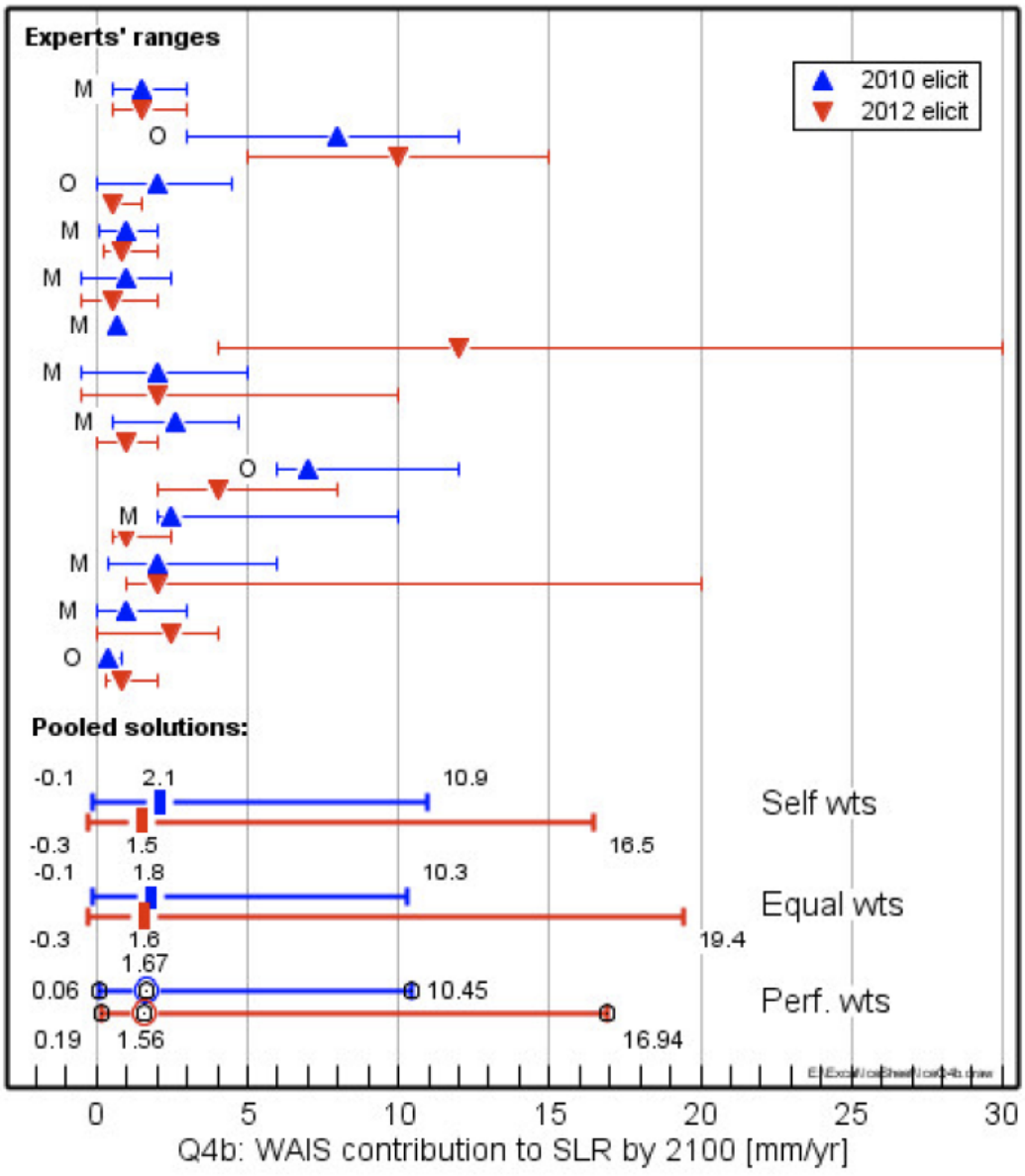

(Above) Figure 7 in the Supplemental Materials of Bamber and Aspinall (2013) whose upper bound was used by NPCC (2015). This range graph plot (lower, upper and best estimate values) shows the individual responses by experts to the survey question (Q4b) on the rate of SLR due to West Antarctic Ice Sheet (WAIS) melting in the 2010 survey (blue) and repeat 2012 survey (red). Also shown are the pooled estimates based on self weighting ("confidence"

multiplied by “expertise”), equal weights and performance weighting.

BA13 also said in the paper that "It (survey) is not a substitute for improved process understanding; nor is it intended to remove uncertainty, but rather to quantify it, given limitations in available information." The BA13 number is not meant to substitute for the process-level projection that NYS RISE or IPCC AR5 projections.

A recent paper by Kopp et al. (2014) also commented on the BA13 upper limit, which attempted to reconcile several available SLR projections. It concluded that:

> " For AIS (Antarctic Ice Sheet), the reconciled RCP 8.5 projections (median/*likely*/*very likely* [90% probability] of 4/−8 to 15/−11 to 33 cm) are significantly reduced in range relative to BA13 (Barmer and Asponall 2013) (median/*likely*/*very likely* of 13/2 to 41/−2 to 83 cm)".

The 90th percentile upper bound in Kopp et al. (2014) is 50 cm lower than the upper bound in Barmer and Asponall (2013). This 50 cm difference from the Antarctic ice sheet can account for a significant fraction of the difference in the projections by NYS RISE and NPCC (2015).

It should be also pointed out that the Appendix IIB of NPCC (2015), which describes the NPCC SLR projection method, does not contain enough details for us to reproduce and evaluate the components in its 75-inch SLR projection.

ClimAID Projection by NPCC (2011)

The ClimAID 2011 report (Horton et al. 2011) projected SLR in NYC for 2050s and 2080s for the central range of 67%. The range with consideration of ice melting is 41 to 55 inches for 2080s. It did not report the value for year 2100. Since the 83th percentile upper bound of 55 inches by ClimaAID (2011) for the period of 2080s is very close to the 90th percentile upper bound of 58 inches for the same period by NPCC (2015), we infer that the SLR in 2100 by using the ClimAID (2011) method would be similar to the NPCC (2015) projection, more than 70 inches for NYC.

ClimAID used very different method to calculate SLR. This is described in Rosenzweig et al (2011) (Page 42, Appendix A) as follows:

> “Around 21,000 to 20,000 years ago, sea level began to rise from its low of about 394 feet below current levels. It approached present-day levels about 8,000 to 7,000 years ago (Peltier and Fairbanks, 2006; Fairbanks, 1989). Most of the rise was accomplished within a 12,000–10,000 year period; thus, the average rate of sea level rise over this period ranged between 0.39 and 0.47 inch per year.” “Thus, the average present-day ice melt rate of 0.04 inch per year during the 2000– 2004 base period is assumed to increase to 0.39 to 0.47 inch per year (all ice melt) by 2100. An exponential curve is then fitted to three points: 2000, 2002 (midpoint of the 2000–2004 base period), and 2100.”

The formula is: (394 feet) divided by 10,000 and 12,000 years to get the range of 0.39 to 0.47 inch/year of SLR from ice at the end of the 21th Century. Since the historical glaciation cycle was

driven by astronomical causes, and deglaciation already ended about 8000 years ago, we think that applying the rate from the past deglaciation cycle is not scientifically justified. There are other differences in the calculations of various contributions to the SLR between our method and the ClimAID study, but because the quantitative details of the ClimAID calculation are not available to us, they are not assessed here.

Finally, the ClimAID (Horton et al. 2011) and the NPCC (2015) used the reference period of 2000 to 2004, while this report used the reference period of 1986-2006 to be consistent with IPCC AR5. The 6-year difference period should add approximately another inch to the NPCC (2015) values if they used the same reference period. Additionally, ClimAID (2011) and NPCC (2015) used a combination of the low emission climate change scenario RCP4.5 and the high emission climate change scenario RCP8.5 in deriving their upper 90^{th} percentile bounds of SLR, while we used the high emission scenario RCP8.5 in calculating the upper 95^{th} percentile bound. These differences in calculation conventions, if removed, will make the difference of ClimAID (2011) and NPCC (2015) SLR projection with our projection even larger.

These differences of the calculations of the upper bound of SLR between NPCC (2011, 2015) and our projection, as well as the similarities among IPCC AR5, Kopp et al. (2014) and our results, led us to conclude that the 75-inch SLR projection for NYC in 2100 by NPCC (2011, 2015) is very likely exaggerated.

Appendix: Sea-Level Rise in NY in the 20th Century

Sea-level rise in Nassau and Suffolk in the past century is calculated using tidal gauge stations located in Battery Park in New York City (NYC), and Montauk in Suffolk County. Sea-level rise has averaged about 1.1 inches per decade since 1900 in NYC and Montauk (Figure A.1). These trends are larger than the observed global rate of sea-level rise, which is 0.7 inches per decade over a similar time period (Church and White, 2011). The relatively larger values are consistent with the GIA effect and the ocean dynamics effect in Section 1. The ratio of SLR in NY to the global mean in the 20th Century is comparable to the ratio projected for the 21st Century. The SLR values also suggest that the GIA contribution is smaller than the upper bound which alone is larger than 0.7 inches per decade as shown in Section 2 (Figure 2.10).

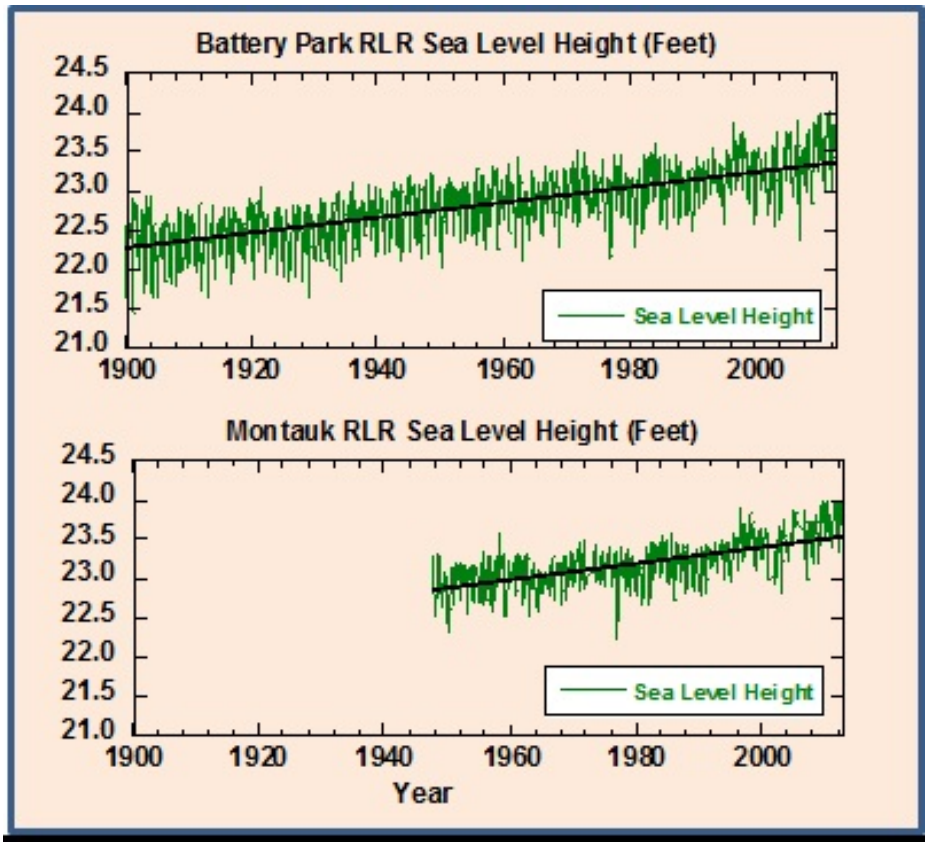

Figure A.1 (above): Monthly mean sea-level height from The Permanent Service for Mean Sea Level (data from Permanent Service for Mean Sea Level (PSMSL): http://www.psmsl.org/).

REFERENCES

Bamber, J.L. & W.P. Aspinall. 2013. An expert judgment assessment of future sea level rise from the ice sheets. Nature Clim. Change 3: 424–427.

Bengtsson, L., S. Koumoutsaris, and K. Hodges, 2011: Large-scale surface mass balance of ice sheets from a comprehensive atmosphere model. Surv. Geophys., **32**, 459–474.

Church, J. A., and N. J. White, 2011: Sea level rise from the late 19th to the early 21st century. Surveys in Geophysics, 32, 585-602.

Church, J. A. et al., 2013: Sea level change, in Climate Change 2013: The Physical Science Basis, IPCC, Chapter 13, Cambridge University Press

Fettweis, X., B. Franco, M. Tedesco, J. H. van Angelen, J. T. M. Lenaerts, M. R. van den Broeke, and H. Gallee, 2013: Estimating Greenland ice sheet surface mass balance contribution to future sea level rise using the regional atmospheric model MAR. Cryosphere, 7, 469–489.

Horton, Radley, Daniel Bader, Lee Tryhorn, Art DeGaetano and Cynthia Rosenzweig, 2011, Climate Risks, Chapter 1 in *Responding to Climate Change in New York State: The ClimAID Integrated Assessment for Effective Climate Change Adaptation by Rosenzweig et al. 2011*. Technical Report 11-18. New York State Energy Research and Development Authority (NYSERDA), Albany, New York (http://www.nyserda.ny.gov/climaid).

Horton, R., C. Little, V. Gornitz, D. Bader, and M. Oppenheimer, 2015: New York City Panel on Climate Change 2015 Report: Sea level rise and coastal storms. Ann. New York Acad. Sci., 1336, 36-44, doi:10.1111/nyas.12593.

Intergovernmental Panel on Climate Change, 2013: Managing the Risks of Extreme Events and Disasters to Advance Climate Change Adaptation. A Special Report of Working Groups I and II of the Intergovernmental Panel on Climate Change [Field, C.B., V. Barros, T.F. Stocker, D. Qin, D.J. Dokken, K.L. Ebi, M.D. Mastrandrea, K.J. Mach, G.-K. Plattner, S.K. Allen, M. Tignor, and P.M. Midgley (eds.)]. Cambridge University Press, Cambridge, UK, and New York, NY, USA, 582 pp.

Kopp, R.E., R.M. Horton, C.M. Little, J.X. Mitrovica, M. Oppenheimer, D.J. Rasmussen, B.H. Strauss, and C. Tebaldi, 2014: Probabilistic 21st and 22nd century sea-level projections at a global network of tide-gauge sites. Earth's Future, 2, no. 8, 383-406, doi:10.1002/2014EF000239.

Konikow, L. F., 2011: Contribution of global groundwater depletion since 1900 to sea-level rise. Geophys. Res. Lett., 38, L17401.

Lambeck, K., C. Smither, and P. Johnston, 1998: Sea-level change, glacial rebound and mantle viscosity for northern Europe. Geophys. J. Int., 134, 102–144.

Little, C. M., N. M. Urban, and M. Oppenheimer, 2013b: Probabilistic framework for assessing the ice sheet contribution to sea level change. Proc. Natl. Acad. Sci. U.S.A., 110, 3264–3269.

New York City Panel on Climate Change (NPCC), 2015: Appendix IIB. Sea level observations and projections: Methods and analyses. . Ann. New York Acad. Sci., 1336, doi:10.1111/nyas.12593.

Peltier, W. R., 2004: Global glacial isostasy and the surface of the ice-age earth: The ICE-5G (VM2) model and GRACE. Annu. Rev. Earth Planet. Sci., 32, 111–149.

Radić, V, Hock, R (2011) Regionally differentiated contribution of mountain glaciers and ice caps to future sea-level rise. Nat Geosci 4: pp. 91-94.

Rosenzweig, C., W. Solecki, A. DeGaetano, M. O'Grady, S. Hassol, P. Grabhorn (Eds.). 2011. *Responding to Climate Change in New York State: The ClimAID Integrated Assessment for Effective Climate Change Adaptation*. Technical Report. New York State Energy Research and Development Authority (NYSERDA), Albany, New York. www.nyserda.ny.gov

Spada, G., and Stocchi, P., 2006. The Sea Level Equation, Theory and Numerical Examples, Aracne, Roma, p. 96, ISBN: 88–548–0384–7.

Taylor, K. E., R. J. Stouffer, and G. A. Meehl, 2012: An overview of CMIP5 and the experiment design. Bulletin of the American Meteorological Society, 93, 485-498.

Van Vuuren, D. and Co-Authors, 2011: The representative concentration pathways: an overview. Climatic Change, 109(1-2), 5-31.

Vaughan, D.G., J.C. Comiso, I. Allison, J. Carrasco, G. Kaser, R. Kwok, P. Mote, T. Murray, F. Paul, J. Ren, E. Rignot, O. Solomina, K. Steffen and T. Zhang, 2013: Observations: Cryosphere. In: Climate Change 2013: The Physical Science Basis. Contribution of Working Group I to the Fifth Assessment Report of the Intergovernmental Panel on Climate Change [Stocker, T.F., D. Qin, G.-K. Plattner, M. Tignor, S.K. Allen, J. Boschung, A. Nauels, Y. Xia, V. Bex and P.M. Midgley (eds.)]. Cambridge University Press, Cambridge, United Kingdom and New York, NY, USA.

Wada, Y., L. P. H. van Beek, F. C. S. Weiland, B. F. Chao, Y. H. Wu, and M. F. P. Bierkens, 2012: Past and future contribution of global groundwater depletion to sea-level rise. Geophys. Res. Lett., 39, L09402.

Zhang, M., Bokuniewicz, H., Lin, W., Jang, S.G., and Liu, P., 2014: Climate Risk Report for Nassau and Suffolk, New York State Resilience Institute for Storms and Emergencies (NYS RISE), NYS RISE Technical Report (in revision) TR-0-14-01, 49 pp (available at www.nysrise.org).

Author Contact Information:

Minghua Zhang, Ph.D
Dean and Director
Professor of Atmospheric Sciences
School of Marine and Atmospheric Sciences
Stony Brook University
Stony Brook, NY 11794-5000
Email: minghua.zhang@stonybrook.edu
Tel: 631-632-8781, Fax: 631-632-8915

Citation to this report:
Zhang, Minghua, Sea-level rise in New York in the 21st Century: Projection and methodology, New York State Resilience Institute for Storms and Emergencies (NYS RISE), NYS RISE Technical Report TR-0-15-01, 29 pp (to be available at http://nysrise.org/news/reports/).

Disclaimer:
Results in this report reflect the opinions of the authors, not of the sponsor or the institutions of the authors. This research is sponsored by the New York State Governor's Office of Storm Recovery.